Applying Petri nets for the analysis of the GSH-ASC cycle in chloroplasts ⋆

Hermenegilda Macià*, M. Isabel González-Sánchez**, Valentín Valero***, and Edelmira Valero**

* Department of Mathematics, Escuela Superior de Ingeniería Informática. Albacete. University of de Castilla-La Mancha. Spain
* Department of Physical Chemistry, Escuela de Ingenieros Industriales. Albacete. University of Castilla-La Mancha. Spain
***Department of Computer Science, Escuela Superior de Ingeniería Informática. Albacete. University of Castilla-La Mancha. Spain
{Hermenegilda.Macia, MIsabel.Gonzalez, Valentin.Valero, Edelmira.Valero}@uclm.es

Keywords: Petri nets, metabolic pathways, biological systems.

Abstract. Petri nets are a useful framework for the analysis of biological systems in various complementary ways, integrating both qualitative and quantitative studies. We apply this formalism to the Glutathione Ascorbate Redox cycle (GSH-ASC) in chloroplasts case study, considering structural Petri net techniques from standard Petri nets to validate the model and to infer new properties, as well as continuous Petri nets in order to have a behavior prediction. In this way, from the continuous Petri net representation we can analyze its behavior under oxidative stress conditions, and from the standard Petri net we can identify some state-conserving or mass-conserving properties.

1 Introduction

Petri nets [8, 10] are a well-known mathematical formalism for the modeling and analysis of concurrent systems. They were introduced by Carl A. Petri [11] in the early 60's. Since this time, they have been extended and applied to several areas [4] such as manufacturing systems, workflow management, telecommunications, communication protocols, etc. Some reasons for using Petri nets are the following: it is easy to describe concurrency and they have a rigorous formal semantics, i.e., their behavior is defined in a precise and unambiguous manner. Additionally, one of the main features of Petri nets is that they have a graphical nature, i.e., you can early get a good knowledge of the system by simple inspection of the Petri net model that represents the system. But, most importantly, there are many tools [21] supporting the model, not only to provide the capability to

⋆ Supported by the Spanish government (cofinanced by FEDER founds) with the project TIN2009-14312-C02-02, and the JCCM regional projects PEII09-0232-7745, PAI-08-0175-8618 and POII10-0235-8597

Recent Advances in Petri Nets and Concurrency, S. Donatelli, J. Kleijn, R.J. Machado, J.M. Fernandes (eds.), CEUR Workshop Proceedings, ISSN 1613-0073, Jan/2012, pp. 119–133.

create or edit Petri net models, but also to simulate the system evolution and even to analyze some properties of interest. Then, there has been an intensive research in the area of Petri nets in the last 40 years to extend the basic model by including some additional features that are of special interest in some specific application domains. Thus, timed and probabilistic extensions of the basic model have been defined [20, 7], as well as continuous and hybrid Petri nets [1]. The application of Petri nets to the description of chemical processes was already proposed by Carl A. Petri in the 70's [12]. In the 90's Reddy et al. [14] were the first who applied Petri nets to the modeling and analysis of metabolic pathways. Nowadays, there are several different extensions of Petri nets for modeling and simulating biological systems, depending on the specifics of the particular chemical processes described (see [9]). A rich framework for modeling and analyzing biochemical pathways which unifies the qualitative, stochastic and continuous paradigms using Petri nets can be found in [3].

In this paper we consider the GSH-ASC cycle in chloroplasts, which is described and analyzed by using continuous and standard Petri nets. Thus, the main goals of this paper can be summarized as follows:

(i) The application of continuous Petri nets to this specific biological process, which provides us with a graphical representation of this chemical process, which becomes easier to modify and analyze than the corresponding (equivalent) ODE, which can be found in [17].
(ii) The application of the classical theory and tools of Petri nets (in the discrete Petri net), and specifically in this paper the structural theory in order to get a better understanding of the biological model and conclude the relationship between the structural elements (invariants) of the underlying discrete Petri net with the chemical properties of this biological process.

There are two models of the GSH-ASC cycle in the literature: Polle's model [13] and the ours one [17]. Polle's model has some shortcomings that were discussed and improved in our paper. The PN model here described for the GSH-ASC cycle in the continuous case was validated by checking that the same results were obtained with the ODE case [17], as indicated in the (i) goal of the present paper.

The outline of the paper is as follows. Section 2 contains a brief description of the GSH-ASC cycle in chloroplasts. In Section 3 we study the dynamic behavior of this biological model by using continuous Petri nets. Then, the structural qualitative study is presented in Section 4, and finally, the conclusions and hints for future research are presented in section 5.

2 The Biological Model

The glutathione-ascorbate redox (GSH-ASC) pathway in chloroplasts is a complex network of spontaneous, photochemical, and enzymatic reactions for detoxifying hydrogen peroxide. In brief, superoxide dismutase (SOD) acts as the first

line of defense, dismutating superoxide radical (O_2^-) to H_2O_2 and O_2. In chloroplasts, H_2O_2 thus generated is reduced to water by ascorbate (ASC) catalyzed with L-ascorbate peroxidase (APX). This is the first step of the GSH-ASC cycle, producing monodehydroascorbate radicals (MDA), which spontaneously disproportionate to ASC and dehydroascorbate (DHA). The next step in the cycle is the regeneration of ASC by glutathione (GSH) either enzymatically catalyzed by glutathione dehydrogenase ($DHAR$) or chemically but a too slow rate to account for the observed photoreduction of DHA in chloroplasts. Lastly, the redox cycle is closed by the regeneration of GSH catalyzed by glutathione reductase (GR) at the expense of photoproduced $NADPH$. These steps are captured by the continuous Petri net model depicted in Figure 1, which provides us with a graphical representation of this biological process.

Tables 1-5 provide mathematical expressions for rate equations as well as the conditions (rate constants and initial concentrations) used for the mathematical modeling of the pathway. Due to the lack of space we omit a detailed description of this metabolic pathway, which can be found in [17], which contains a supplementary material section devoted to this description.

It is very difficult to validate numerical data here shown against real biological data. The metabolic pathway under study includes four enzymatic steps and a complex set of photochemical and spontaneous chemical reactions, which is not possible to implement under "in vitro" conditions so that data from Figures 2 and 3 can be tested in an experimental way in the laboratory. However, the values of the kinetic constants and initial conditions used to run the model (Tables 4 and 5) have been taken, when possible, from data reported in the scientific literature, obtained with real systems. APX does not appear on Table 2 because of it has not been considered under steady-state conditions, since it is the most hydrogen peroxide sensitive enzyme in the pathway. Instead, we have introduced its catalytic mechanism including a stage of inactivation by excess of hydrogen peroxide and a stage of de novo synthesis of the protein, which gives the cell the opportunity to recover the amount of APX inactivated, which represents one of the main defense mechanisms of plants to mitigate oxidative stress.

Table 1. Chemical reactions involved in the cycle which have been introduced in the model and notation used for their respective apparent bimolecular rate constants

Reaction	Notation Reaction
$MDA + MDA \rightarrow ASC + DHA$	k_1
$DHA + 2\ GSH \rightarrow ASC + GSSG$	k_4
$2\ O_2^- + 2\ H^+ \rightarrow O_2 + H_2O_2$	k_5
$O_2^- + ASC \rightarrow H_2O_2 + MDA$	k_6
$O_2^- + 2\ GSH \rightarrow H_2O_2 + GSSG$	k_7
$H_2O_2 + 2\ ASC \rightarrow 2\ H_2O + 2\ MDA$	k_8

Table 2. Chemical reactions involved in the APX mechanism

Reaction	Notation Reaction
$APX + H_2O_2 \rightarrow CoI + H_2O$	k_1^{APX}
$CoI + ASC \rightarrow CoII + MDA$	k_2^{APX}
$CoII + ASC \rightarrow APX + MDA$	k_3^{APX}
$CoI + H_2O_2 \rightarrow APX_i$	k_4^{APX}
synthesis de novo of APX	k_5^{APX}

Table 3. Steady-state rate equations used for the enzymes involved in the model

Enzyme	Rate equation
SOD	$k_{SOD}[SOD]_0[O_2^-]$
DHAR	$\frac{k_{cat}^{DHAR}[DHAR]_0[DHA][GSH]}{K_i^{DHA}K_M^{GSH1} + K_M^{DHA}[GSH] + (K_M^{GSH1} + K_M^{GSH2})[DHA] + [DHA][GSH]}$
GR	$\frac{k_{cat}^{GR}[GR]_0[NADPH][GSSG]}{K_M^{NADPH}[GSSG] + K_M^{GSSG}[NADPH] + [NADPH][GSSG]}$

Table 4. List of kinetic constants values used to simulate the model under "standard" conditions.

F	640	k_{cat}^{GR}	595	k_{cat}^{DHAR}	142	k_{SOD}	200	k_1^{APX}	12	k_2^{APX}	50
k_3^{APX}	2.1	k_4^{APX}	0.7	k_5^{APX}	0.01	k_1	0.5	k_4	0.1	k_5	0.2
k_6	0.2	k_7	0.7	k_8	$2E-6$	k_{12}	1.3	k_{13}	42.5	k_N	0.5
K_M^{NADPH}	3	K_M^{GSSG}	200	K_M^{GSH}	2500	K	$5E5$				

Table 5. List of (non-zero) initial concentrations used to simulate the model under "standard" conditions.

Enzymes	Initial concentration (μM)	Species	Initial concentration (μM)
GR	1.4	APX	70
DHAR	1.7	NADPH	150
SOD	50	GSH	4000
		ASC	10000

3 Continuous Petri Nets

We use continuous Petri nets [1], for which places no longer contain integer values, but positive real numbers, and transitions fire in a continuous way. Semantics

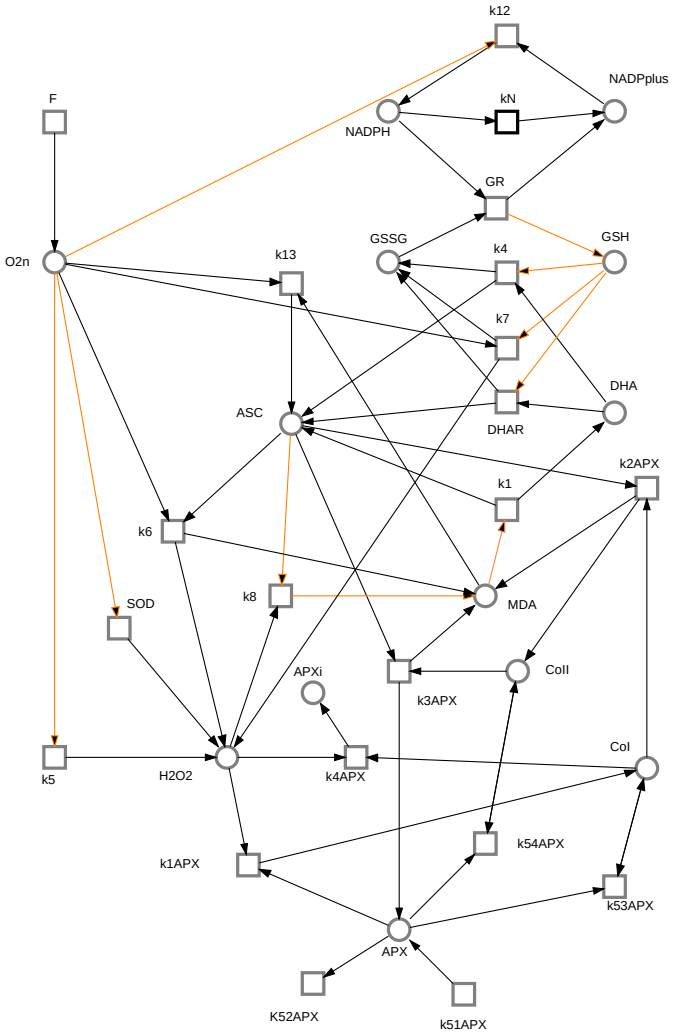

Fig. 1. Continuous Petri net model for the GSH-ASC cycle (orange arcs have weight 2)

of continuous Petri Nets is then defined by means of a system of Ordinary Differential Equations [2]. The continuous Petri net model for the GSH-ASC cycle is that shown in Figure 1 (obtained using the Snoopy tool [16]). This model has been obtained by adapting the biological process described in [17], according to the following considerations:

1. $[CO_2]$ is considered constant, so that the flux of NADPH consumption by the Calvin cycle (and other electron-consuming reactions) is $k_N = k'_N\,[CO_2]$.

2. The synthesis de novo of APX in [17] is considered as $k_5^{APX}([APX]_0 - [APX] - [CoI] - [CoII])$. Then, read arcs are used for CoI and $CoII$ places, since even if k_5^{APX} does not appear in their corresponding equations, it is included in the APX equation. We have then considered four new transitions in the continuous Petri net model, with the following associated kinetic constants: $k51APX$ with $k_5^{APX}[APX_0]$, and $k5APX2$, $k5APX3$ and $k5APX4$ with k_5^{APX}.
3. There is a constant electron source in the model, F, whose flux is divided among three competitive routes: the photoproduction of O_2^- (transition $k5$), the photoreduction of $NADP^+$ (transition $k12$) and the photoreduction of MDA (transition $k13$).

The corresponding ODEs for this continuous Petri net model are those shown in Table 6, which consist of 13 molecular species and 21 reactions defining the equations. These are the same ODEs that we obtained in [17] (supplementary material).

Table 6. Differential equations system

$$\frac{d[NADPH]}{dt} = -v_{GR} - k'_N[CO_2][NADPH] + k_{12}[NADP^+] \quad (1)$$

$$\frac{d[NADP^+]}{dt} = v_{GR} + k'_N[CO_2][NADPH] - k_{12}[NADP^+] \quad (2)$$

$$\frac{d[GSH]}{dt} = 2\,(\,v_{GR} - v_{DHAR} - k_7[O2^-][GSH] - k_4[DHA][GSH]\,) \quad (3)$$

$$\frac{d[GSSG]}{dt} = -v_{GR} + v_{DHAR} + k_7[O2^-][GSH] + k_4[DHA][GSH] \quad (4)$$

$$\begin{aligned}\frac{d[ASC]}{dt} = {} & v_{DHAR} + k_1[MDA]^2 + k_4[DHA][GSH] + k_{13}[MDA] \\ & - k_2^{APX}[ASC][CoI] - k_3^{APX}[ASC][CoII] - k_6[O2^-][ASC] \\ & - 2\,k_8[H_2O_2][ASC]\end{aligned} \quad (5)$$

$$\frac{d[DHA]}{dt} = -v_{DHAR} + k_1[MDA]^2 - k_4[DHA][GSH] \quad (6)$$

$$\begin{aligned}\frac{d[MDA]}{dt} = {} & k_2^{APX}[ASC][CoI] + k_3^{APX}[ASC][CoII] - 2\,k_1[MDA]^2 \\ & + k_6[O_2^-][ASC] + 2\,k_8[H_2O_2][ASC] - k_{13}[MDA]\end{aligned} \quad (7)$$

$$\begin{aligned}\frac{d[H_2O_2]}{dt} = {} & v_{SOD} - k_1^{APX}[H_2O_2][APX] - k_4^{APX}[H_2O_2][CoI] + k_5[O_2^-]^2 \\ & + k_6[O_2^-][ASC] + k_7[O2^-][GSH] - k_8[H_2O_2][ASC]\end{aligned} \quad (8)$$

$$\begin{aligned}\frac{d[APX]}{dt} = {} & -k_1^{APX}[H_2O_2][APX] + k_3^{APX}[ASC][CoII] \\ & + k_5^{APX}([APX]_0 - [APX] - [CoI] - [CoII])\end{aligned} \quad (9)$$

$$\frac{d[CoI]}{dt} = k_1^{APX}[H_2O_2][APX] - k_2^{APX}[ASC][CoI] - k_4^{APX}[H_2O_2][CoI] \quad (10)$$

$$\frac{d[CoII]}{dt} = k_2^{APX}[ASC][CoI] - k_3^{APX}[ASC][CoII] \quad (11)$$

$$\frac{d[APX_i]}{dt} = k_4^{APX}[H_2O_2][CoI] \quad (12)$$

$$\begin{aligned}\frac{d[O_2^-]}{dt} = {} & -2\,v_{SOD} + F - 2\,k_{12}[NADP^+] - 2\,k_5[O_2^-]^2 \\ & - k_6[O_2^-][ASC] - k_7[O2^-][GSH] - k_{13}[MDA]\end{aligned} \quad (13)$$

As a consequence of the photoreduction explained above, the recovery of the reducing power is variable and dependent on the $NADP^+$ and MDA concentrations present in chloroplasts. This provides a great flexibility to the model and a greater ability to study stress conditions. The next values have been used for F:

(i) Unstressed chloroplasts, $F = 640$, giving a production rate of of 222.2 Ms^{-1}, which is within the range previously mentioned in chloroplasts (Figure 2); under these conditions, a steady state was rapidly achieved by the system, in which metabolite concentrations and fluxes remained constant.

(ii) Stressed chloroplasts, $F = 2400$ (intense light exposure), which gives rise to APX photoinactivation (Figure 3); under these conditions, the antioxidant concentration in the chloroplast gradually decreased, in the order NADPH, GSH and ASC, so that their respective oxidized species concentrations increased. The disappearance of ASC was followed by the rapid inactivation of APX, reflecting what occurs in reality, accompanied by a sharp increase in APXi and H_2O_2.

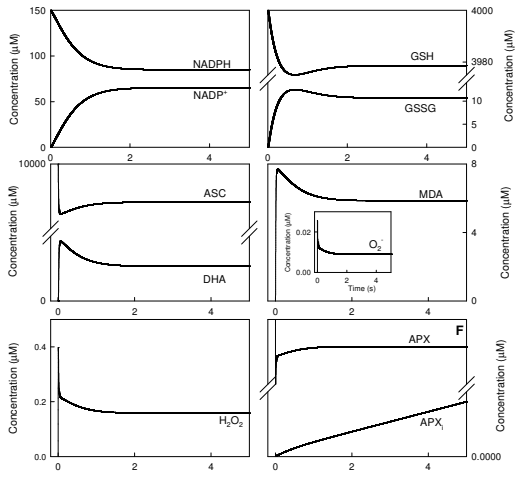

Fig. 2. Simulated progress curves corresponding to the species involved in the mechanism with $F = 640$

4 Structural Analysis

In this section we apply the classical structural techniques on Petri nets [10] in order to verify and analyze the metabolic pathway. For that purpose we build a discrete Petri net model (see Figure 4) from the description of the cycle following the steps described in [2]. We can remove the read arcs (also called test arcs)

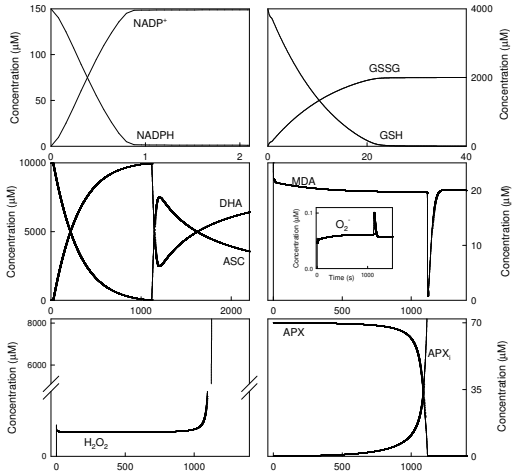

Fig. 3. Simulated progress curves corresponding to the species involved in the mechanism with $F = 2400$

from the continuous Petri net of Figure 1, since they are irrelevant in the corresponding incidence matrix, and therefore in the structural analysis. We then join the transitions *k52APX*, *k53APX* and *k54APX* into a single output transition from *APX*, named *k5APXo*, and we also rename the input transition *k51APX* by *k5APXi*. On the other hand, in order to identify the I/O behavior we add a new place that represents the water generated by the reactions (transitions) *k4APX* and *k1APX*, and a new transition (*outwater*) that models the water self control of chloroplasts.

The obtained Petri net has been analyzed by using a well known Petri net tool, Charlie [15], which allows us to obtain the corresponding invariants for this Petri net.

4.1 P-invariants

A P-invariant defines a mass conservation law and has associated its corresponding biological interpretation. In this case we have obtained three P-invariants (Table 7).

Table 7. P-invariants

$P - inv_1 =$ { NADPH, $NADP^+$ }
$P - inv_2 =$ { 2 GSSG, GSH }
$P - inv_3 =$ { ASC, DHA, MDA }

This means that the pathway under study consists of three moiety-conserved cycles coupled in series to attain a very high amplification capacity [18] against an increase in hydrogen peroxide concentration. In its evolution, since the appearance of oxygen in the atmosphere, the cell has developed a very efficient defense

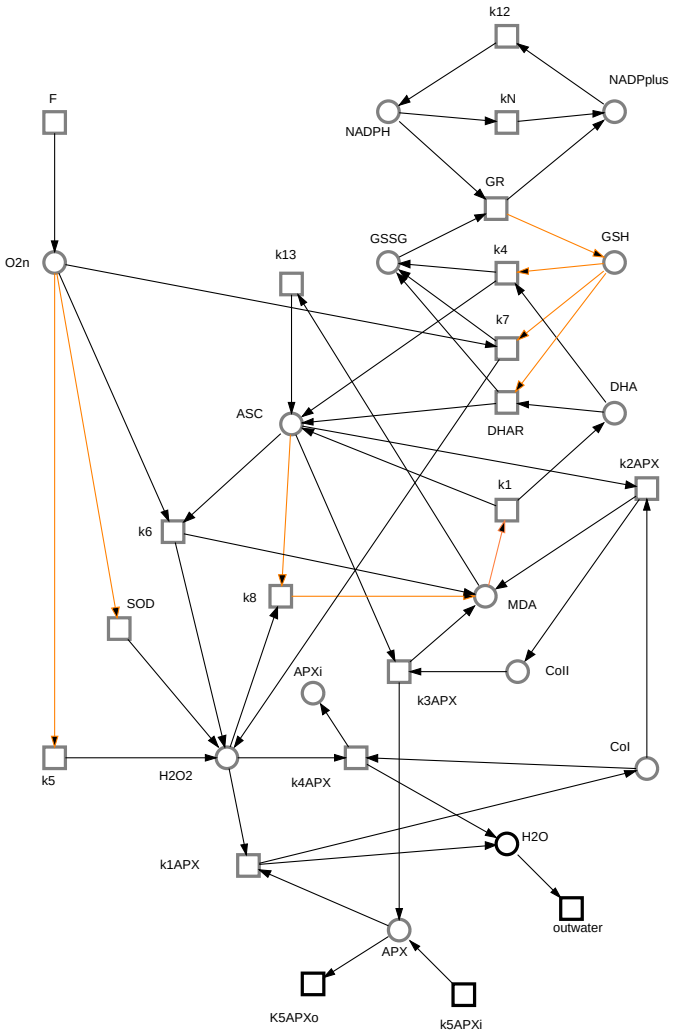

Fig. 4. Petri net model for the GSH-ASC cycle (orange arcs are of weight 2)

tool against oxygen toxicity, although it needs a continuous supply of NADPH. Observe that for each P-invariant there must be a non-zero initial concentration spread along its places, otherwise these places would remain unmarked forever.

(i) $P - inv_1$ captures the consumption of $NADPH$ by the Calvin cycle and GR, and its corresponding recovery in daylight.

(ii) $P - inv_2$ corresponds to the glutahione pool in chloroplasts involving the enzymes GR and $DHAR$. Spontaneous oxidation of GSH in the presence of DHA and O_2^- is also included.

(iii) $P - inv_3$ is related to the interconversion of ASC both spontaneously and catalyzed by $DHAR$ and APX.

4.2 T-invariants

A T-invariant defines a state-conserving subnetwork and has associated its corresponding biological interpretation. In our case (Table 8), using again the Charlie tool, there are 26 minimal semipositive transition invariants.

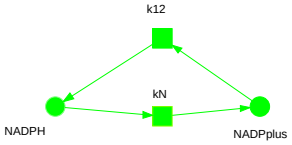

Fig. 5. $T - inv_2$

Let us see a brief description of some of them:

(i) $T - inv_2$ (Fig. 5) is a trivial T-invariant. These transitions capture a reversible reaction, each one modeling a direction in this reaction. Biologically speaking, it corresponds to the consumption and regeneration of $NADPH$ in the two stages of the photosynthesis.

(ii) $T - inv_6$ (Fig. 6) represents in a very clear way the removal of O_2^- and H_2O_2 (reactive oxygen species) by reaction with the reducing agents GSH and ASC, at the expense of the reducing power of $NADPH$.

(iii) $T - inv_7$ (Fig. 6) refers to the catalytic cycle of APX.

(iv) $T - inv_{15}$ (Fig. 7) represents the removal of O_2^- by its spontaneous reduction to H_2O_2 in the presence of ASC, the subsequent removal of H_2O_2 by the catalytic cycle of APX, and the recovery of ASC through the substrate cyclying of GSH and $NADPH$.

(v) $T - inv_{24}$ (Fig. 7) is a reflection of the enzymatic steps involved in the pathway: SOD, GR, $DHAR$ and APX.

Another advantage of the Petri net representation is that it can be easily modified for modeling different situations. For instance, in order to consider the same cycle in dark conditions, we only have to remove in Figure 4 the transition F. Then, if we now apply structural analysis we obtain the same three P-invariants, but we only obtain the two first T-invariants, $T - inv_1$ and $T - inv_2$, which are the input (synthesis *de novo*) and output (inactive enzyme) of APX, and the two stages of photosynthesis.

Table 8. T-invariants

T-invariant	Transitions/Reactions (number of fires)
$T - inv_1$	k5APXo (1), k5APXi (1)
$T - inv_2$	kN (1), k12 (1)
$T - inv_3$	k13 (3),k6 (1), k8 (1), F (1)
$T - inv_4$	k13 (2), k8 (1), SOD (1), F (2)
$T - inv_5$	k13 (2), k8 (1), k5 (1), F (2)
$T - inv_6$	GR (1), k12 (1), k7 (1), k13 (2), k8 (1), F (1)
$T - inv_7$	k13 (3), k2APX (1), k3APX (1), k6(1), k1APX (1), F (1), outwater (1)
$T - inv_8$	k13 (2), k2APX (1), k3APX (1), SOD (1), k1APX (1), F (2), outwater (1)
$T - inv_9$	k13 (2), k2APX (1), k3APX (1),k5 (1), k1APX (1),F (2), outwater (1)
$T - inv_{10}$	GR (1), k12 (1), k7 (1), k13 (2), k2APX (1), k3APX(1), k1APX (1), F (1), outwater (1)
$T - inv_{11}$	GR (3), k12 (3), k4 (3), k1 (3), k6 (2), k8 (2), F (2)
$T - inv_{12}$	GR (1), k12 (1), k4 (1), k1 (1), k8 (1), SOD (1), F (2)
$T - inv_{13}$	GR (1), k12 (1), k4 (1), k1 (1), k8 (1), k5 (1), F (2)
$T - inv_{14}$	GR (2), k12 (2), k4 (1), k7 (1), k1 (1), k8 (1), F (1)
$T - inv_{15}$	GR (3), k12 (3), k4 (3), k1 (3), k2APX (2), k3APX (2), k6 (2), k1APX (2), F (2), outwater (2)
$T - inv_{16}$	GR (1), k12 (1), k4 (1), k1 (1), k2APX (1), k3APX (1), SOD (1), k1APX (1), F (2), outwater (1)
$T - inv_{17}$	GR (1), k12 (1), k4 (1), k1 (1), k2APX (1), k3APX (1), k5 (1), k1APX (1), F (2), outwater (1)
$T - inv_{18}$	GR (2), k12 (2), k4 (1), k7 (1), k1 (1), k2APX (1), k3APX (1), k1APX (1), F (1), outwater (1)
$T - inv_{19}$	GR (3), k12 (3), DHAR (3), k1 (3), k6 (2), k8 (2), F (2)
$T - inv_{20}$	GR (1), k12 (1), DHAR (1), k1 (1), k8 (1), SOD (1), F (2)
$T - inv_{21}$	GR (1), k12 (1), DHAR (1), k1 (1), k8 (1), k5 (1), F (2)
$T - inv_{22}$	GR (2), k12 (2), k7 (1), DHAR (1), k1 (1), k8 (1), F (1)
$T - inv_{23}$	GR (3), k12 (3), DHAR (3), k1 (3), k2APX (2), k3APX (2), k6 (2), k1APX (2), F (2), outwater (2)
$T - inv_{24}$	GR (1), k12 (1), DHAR (1), k1 (1), k2APX (1), k3APX (1), SOD (1), k1APX (1), F (2), outwater (1)
$T - inv_{25}$	GR (1), k12 (1), DHAR (1), k1 (1), k2APX (1), k3APX (1), k5 (1), k1APX (1), F (2), outwater (1)
$T - inv_{26}$	GR (2), k12 (2), k7 (1), DHAR (1), k1 (1), k2APX (1), k3APX (1), k1APX (1), F (1), outwater (1)

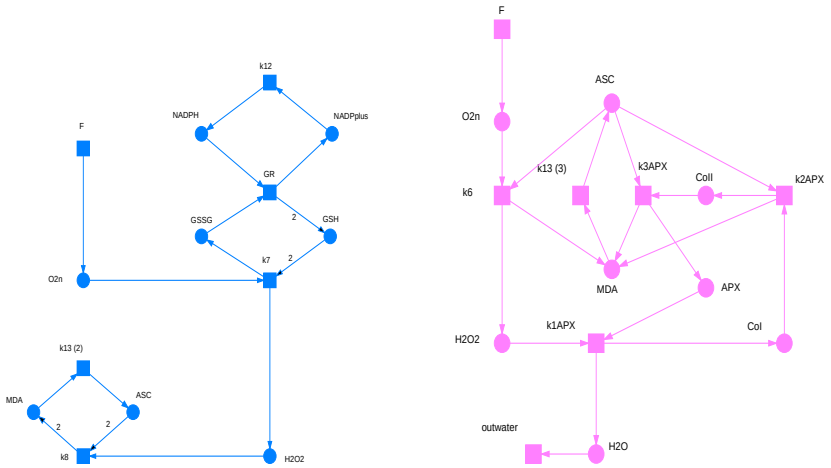

Fig. 6. $T - inv_6$ and $T - inv_7$

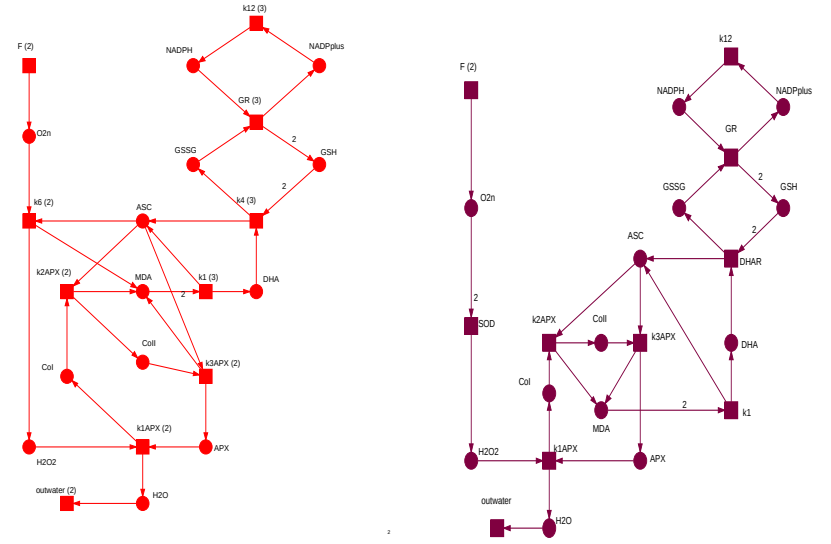

Fig. 7. $T - inv_{15}$ and $T - inv_{24}$

4.3 Core network

We now apply the procedure proposed in [5] in order to identify the core net that represents the network's dynamics. Transition $k4APX$ does not belong to any T-invariant, therefore, it can be removed at the steady-state, together with

the place $APXi$, which becomes isolated upon the removal of $k4APX$. Furthermore, $T - inv_2$ is a trivial T-invariant, so that we can use a macro transition for these transitions. Next, we compute the maximal Abstract Dependent Transition (ADT) sets, considering that two transitions depend on each other if they occur always together in the set of T-invariants. In this case we obtain an only connected ADT set $\{k1APX, k2APX, k3APX\}$, which can also be collapsed in a single macro-transition (together with $T - inv_1$). This coarse network (Figure 8) gives us a reduced vision of the chemical process behavior, so it contributes to attain a better understanding of this process, also allowing us to test the robustness and the identification of the fragile nodes.

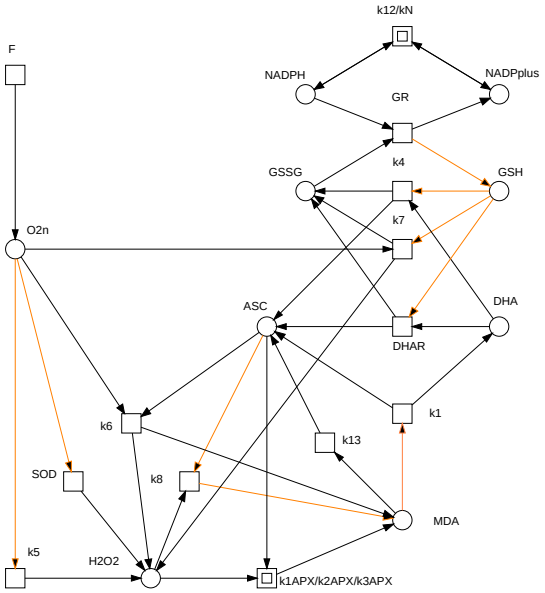

Fig. 8. Coarse Petri net structure of the GSH-ASC cycle

Robustness is defined as the ability of the system to maintain its function against internal and external perturbations [6]. In the pathway under study, robustness is directly related to APX activity [17]. To maintain APX activity, the cell has developed a very efficient defense tool against oxygen toxicity, based on two coupled substrate cycles: *GSH-GSSG* ($P - inv_2$) and *ASC-MDA-DHA* ($P - inv_3$), although it needs a continuous supply of *NADPH* ($P - inv_1$). Substrate cycles are powerful metabolic tools involving two enzymes acting in opposite directions, whereby a target metabolite is reversibly interconverted into another chemical species without being consumed [19]. The physiological expla-

nation proposed for this wasteful cycling is that is mainly a way of amplifying a metabolic response to a change in a metabolic concentration, thus greatly improving the sensitivity of metabolic regulation. The waste of *NADPH* can the be understood as the cost that chloroplasts must pay to swiftly detoxify $H_2\,O_2$ and O_2^-.

It is also very important to analyze the redundancy of a pathway. It is the hallmark of biological networks where the very same function is carried out by different pathways, which provides robustness against perturbations like mutation. In the *GSH-ASC* cycle, if a mutation block *SOD*, there is a parallel spontaneous step for ${O_2}^-$ dismutation (k_5), as can been seen in Figure 8. The same holds for *DHAR* (k_4), in such a way that chloroplasts can recover the reducing power necessary to detoxify reactive oxygen species in the absence of these enzymes. Redundancy of the pathway under study is clearly revealed by comparison of $T - inv_{15}$ and $T - inv_{24}$, which represent the chemical and the enzymatic pathways, respectively, to eliminate H_2O_2.

Another information that is teased out from the coarse network is that *NADPH* is the shared node for two pathways: the *Calvin* cycle and the *GSH-ASC* cycle. If the recovery of *NADPH* is silenced, it results in a complete loss of function of both pathways in the core network indicating that it is indeed the fragile node in the network. The pathway under study is very interesting, since the same day-light that gives rise to O_2^- radicals also generates *NADPH* and *ASC* to detoxify H_2O_2 arising from O_2^- dismutation. Therefore it is very important to know the relative weight of each route in the growth conditions of plants.

5 Conclusions and Future Work

The GSH-ASC cycle in chloroplasts has been modelled using continuous and discrete Petri nets. For that purpose, we have defined the specific continuous Petri net model that corresponds to the network of chemical and enzymatic steps involved in the cycle, and we have studied it in two ways: the quantitative one, which helps us to make a prediction behavior; and the qualitative one, applying structural techniques, considering the core structure. We have obtained their corresponding biological interpretation that help us to understand this biological system.

As future work we intend to add some additional steps into the pathway, which would be helpful to have a better understanding of the biological behavior considering some new features, such as dark-light interactions. We also intend to apply other known formal techniques to the study of the GSH-ASC cycle in chloroplasts, for instance, we may apply model checking techniques in order to conclude whether a certain property is fulfilled or not by the chemical system. Finally, it can also be of interest to derive probabilistic informations from a chemical system, i.e., we can use a probabilistic framework, like stochastic Petri nets (SPNs), for the modeling of the GSH-ASC cycle in chloroplasts, and derive the relevant stochastic information of the system.

References

1. R. David and H. Alla. *Discrete, Continuous and Hybrid Petri Nets*. Springer, 2005.
2. D. Gilbert and M. Heiner. *From Petri Nets to Differential Equations - an Integrative Approach for Biochemical Network Analysis*. Proc. ICATPN 2006, Turku, June, Springer LNCS 4024, pp. 181-200, 2006.
3. D. Gilbert, M. Heiner, and S. Lehrack. *A Unifying Framework for Modelling and Analysing Biochemical Pathways Using Petri Nets*. Proc. of Computational Methods in Systems Biology 2007, CMSB 2007, M. Calder and S. Gilmore (eds), Springer, LNCS/LNBI 4695, pp.200-216, 2007.
4. C. Girault and R. Valk. *Petri Nets for Systems Engineering. A Guide to Modelling, Verification, and Applications*. Springer, 2003.
5. M. Heiner and K. Sriram. *Structural Analysis to Determie the Core of Hypoxia Response Network*. PLoS ONE 5(1): e8600, doi:10.1371/journal.pone.0008600, 2010.
6. H. Kitano. *Biological robustness*. Nature Reviews Genetics, Vol. 5, pp. 826-837, 2004.
7. M. Kudlek. *Probability in Petri Nets*. Fundamenta Informaticae, vol 67,1-3, pp.121-130, 2005.
8. T. Murata. *Petri Nets: Properties, Analysis and Applications*. Poc. of IEEE, vol. 77, 4, pp.541-580, 1989.
9. M. Peleg, D. Rubin, and R.B. Altman. *Using Petri Net Tools to Study Properties and Dynamics of Biological Systems*. Journal of the American Medical, vol 12, 2, pp.181-199, 2005.
10. J.L. Peterson. *Petri Net Theory and the Modeling of Systems*. Prentice-Hall, 1981.
11. C.A. Petri. *Kommunication mit Automaten*. PhD thesis, Schriften des IMN, Institut für Instrumentelle Mathematic, Bonn, 1962.
12. C.A. Petri. *Interpretations of Net Theory*. GMD, Interner Bericht, 2nd improved edition, 1976.
13. A. Polle. *Dissesting the superoxide dismutase-ascorbate-glutathione-pathway in chloroplasts by metaboloc modeling: computer simulations as a step towards flux analysis*. Plant Physiology, Vol. 126, pp. 445-461, 2001.
14. V.N. Reddy, M.L. Mavrovouniotis, and M.N. Liebman. *Petri Net Representation in Metabolic Pathways*. In Proc. First International Conference on Intelligent Systems for Molecular Biology, pp. 328û336, Menlo Park. AAI, 1993.
15. Data Structures University of Technology in Cottbus, Dep. of Computer Science and Software Dependability. *Charlie*. 2010. http://www-dssz.informatik.tu-cottbus.de/.
16. Data Structures University of Technology in Cottbus, Dep. of Computer Science and Software Dependability. *Snoopy*. 2009. http://www-dssz.informatik.tu-cottbus.de/.
17. E. Valero, M. I. González-Sánchez, H. Macià, and F. García-Carmona. *Computer Simulation of the Dynamic Behavior of the Glutathione-Ascorbate Redox Cycle in Chloroplasts*. Plant Physiology, Vol. 149, pp. 1958-1969, 2009.
18. E. Valero, R. Varón, and F. García-Carmona. *Kinetic analysis of a model for double substrate cycling: highly amplified ADP (and/or ATP) quantification*. Biophysical Journal, Vol. 86, pp. 3598-3606, 2004.
19. Valero, E. and Varón, R. and García-Carmona, F. *Kinetics of a self-amplifying substrate cycle: ADP-ATP cycling assay*. Biochem J 350, pp. 237-243, 2000.
20. J. Wang. *Timed Petri nets: theory and application*. Kluwer international series on discrete event dynamic systems, vol.9, 1998.
21. Petri Nets World. *http://www.informatik.uni-hamburg.de/TGI/PetriNets/*.